Brain Structure and Function (2020) 225:853–870
https://doi.org/10.1007/s00429-020-02045-2

ORIGINAL ARTICLE

Thalamic afferents emphasize the different functions of macaque precuneate areas

Michela Gamberini[1] · Lauretta Passarelli[1] · Daniele Impieri[1] · Katrina H. Worthy[2,3] · Kathleen J. Burman[2] · Patrizia Fattori[1] · Claudio Galletti[1] · Marcello G. P. Rosa[2,3] · Sophia Bakola[2,3]

Received: 11 July 2019 / Accepted: 7 February 2020 / Published online: 20 February 2020
© Springer-Verlag GmbH Germany, part of Springer Nature 2020

Abstract

We studied the thalamic afferents to cortical areas in the precuneus using injections of retrograde fluorescent neuronal tracers in four male macaques (*Macaca fascicularis*). Six injections were within the limits of cytoarchitectural area PGm, one in area 31 and one in area PEci. Precuneate areas shared strong input from the posterior thalamus (lateral posterior nucleus and pulvinar complex) and moderate input from the medial, lateral, and intralaminar thalamic regions. Area PGm received strong connections from the subdivisions of the pulvinar linked to association and visual function (the medial and lateral nuclei), whereas areas 31 and PEci received afferents from the oral division of the pulvinar. All three cytoarchitectural areas also received input from subdivisions of the lateral thalamus linked to motor function (ventral lateral and ventral anterior nuclei), with area PEci receiving additional input from a subdivision linked to somatosensory function (ventral posterior lateral nucleus). Finally, only PGm received substantial limbic association afferents, mainly via the lateral dorsal nucleus. These results indicate that area PGm integrates information from visual association, motor and limbic regions of the thalamus, in line with a hypothesized role in spatial cognition, including navigation. By comparison, dorsal precuneate areas (31 and PEci) are more involved in sensorimotor functions, being akin to adjacent areas of the dorsal parietal cortex.

Keywords Dorsal thalamus · Pulvinar · Lateral posterior nucleus · Mediodorsal nucleus · Spatial orientation · Sensorimotor

Abbreviations

Superior or anterior (thalamic nuclei and regional subdivisions)

AD	Anterior Dorsal
AM	Anterior Medial
AV	Anterior Ventral
LD	Lateral Dorsal

Medial (thalamic nuclei and regional subdivisions)

MD	Medial Dorsal
MDdc	Medial Dorsal, densocellular part
MDmc	Medial Dorsal, magnocellular part
MDmc/pc	Medial Dorsal, magnocellular/parvocellular part
MDmf	Medial Dorsal, multiform part
MDpc	Medial Dorsal, parvocellular part

Lateral (thalamic nuclei and regional subdivisions)

VA	Ventral Anterior
VAdc	Ventral Anterior, densocellular part
VAmc	Ventral Anterior, magnocellular part
VApc/dc	Ventral Anterior, parvocellular/densocellular part
VL	Ventral Lateral
VLc	Ventral Lateral, caudal
VLm	Ventral Lateral, medial
VLo	Ventral Lateral, oral
VLps	Ventral Lateral, postrema
VPI	Ventral Posterior Inferior
VPL	Ventral Posterior Lateral
VPLc	Ventral Posterior Lateral, caudal

Michela Gamberini and Lauretta Passarelli have contributed equally to this work, and should be seen as equal first authors, listed here in alphabetical order.

✉ Sophia Bakola
sofia.bakola@monash.edu

[1] Department of Biomedical and Neuromotor Sciences, University of Bologna, 40126 Bologna, Italy

[2] Department of Physiology, Biomedicine Discovery Institute, Monash University, Clayton, VIC 3800, Australia

[3] Australian Research Council, Centre of Excellence for Integrative Brain Function, Monash University Node, Clayton, VIC 3800, Australia

VPLo	Ventral Posterior Lateral, oral
VPM	Ventral Posterior Medial
VPMpc	Ventral Posterior Medial, parvocellular
X	Area X

Intralaminar (thalamic nuclei and regional subdivisions)

CL	Central Lateral
CM	Centromedian
Csl	Central superior lateral
Li	Limitans
Pcn	Paracentral
PF	Parafascicular
SG	Suprageniculate

Periventricular (thalamic nuclei and regional subdivisions)

Cdc	Central densocellular
Cif	Central inferior
Cim	Central intermediate
Clc	Central latocellular
Cs	Central superior
Pa	Paraventricular
Pt	Paratenial
Re	Reuniens

Posterior (thalamic nuclei and regional subdivisions)

LP	Lateral Posterior
Pul	Pulvinar
Pul.i	Pulvinar, inferior subdivision
Pul.l	Pulvinar, lateral subdivision
Pul.m	Pulvinar, medial subdivision
Pul.o	Pulvinar, oral (anterior) subdivision
GLd	Lateral geniculate body, dorsal division
GMmc	Medial geniculate body, magnocellular division
GMpc	Medial geniculate body, parvocellular division

Other (thalamic nuclei and regional subdivisions)

Hlpc	Lateral habenula, parvocellular division
Hm	Medial habenula
R	Reticular
Sm	Stria medullaris
STN	Subthalamic nucleus
THI	Habenulo-interpendicular tract

Cortical areas

SPL	Superior parietal lobule
dr PGm	Area PGm, dorsorostral sector
vc PGm	Area PGm, ventrocaudal sector
V6	Area V6
V6Ad	Area V6A, dorsal portion
V6Av	Area V6A, ventral portion
PEc	Area PEc
PE	Area PE
PEci	Area PE, cingulate portion

Introduction

The term precuneate gyrus (or precuneus) refers to the region of cortex located on the medial surface of the parietal lobe, which is anatomically circumscribed by the parieto-occipital, suprasplenial, and cingulate sulci. Functionally, the precuneus is delimited caudally by visual and visuomotor association cortex (areas V6 and V6A), dorsally by sensorimotor superior parietal areas (PEc, PEci), rostrally by subdivisions of posterior cingulate cortex (area 23 complex), and ventrally by still poorly characterized subdivisions of putative visual cortex (Passarelli et al. 2018). In terms of cytoarchitecture, the precuneus is similarly organized in humans (Vogt and Laureys 2005; Cavanna and Trimble 2006) and monkeys (Morecraft et al. 2004; Vogt et al. 2005), with most of its volume occupied by cytoarchitectural areas PGm and 31.

In humans, the precuneus has been considered a critical component of the brain systems for numerous aspects of cognitive functions, including participation in the network linked to the neural correlates of self-consciousness (Cavanna and Trimble 2006), and has been reported to be particularly affected in cognitive decline linked to aging and dementia (Buckner et al. 2000, 2005; Matsuda 2001; Lustig et al. 2003). According to studies in non-human primates (Olson et al. 1996; Ferraina et al. 1997; Thier and Andersen 1998; Sato et al. 2006, 2010) and humans (Wenderoth et al. 2005; Baumann et al. 2012), the caudal medial cortex, including the precuneate region, emerges as a site where multiple sensorimotor systems interact to guide complex spatial behaviors such as gaze and limb orientation and navigation. Anatomically, there is evidence showing that, in monkeys, the precuneus forms extensive connections with superior and inferior parietal, cingulate, and retrosplenial areas of the cortex, whereas connections with the frontal lobe are somewhat de-emphasized when compared to adjacent superior parietal areas (Pandya and Seltzer 1982; Cavada and Goldman-Rakic 1989a, b; Leichnetz 2001; Parvizi et al. 2006; Passarelli et al. 2018). In this aspect, the precuneus appears to be a node, or intermediary structure, in the parieto-medial temporal pathway with access to the hippocampal and parahippocampal formations, suggesting a role in whole-body movements and spatial memory (Kravitz et al. 2011).

Recent neuroimaging studies in healthy humans have identified functional interactions between the precuneus and the thalamus (Tomasi and Volkow 2011; Zhang and Li 2012; Cunningham et al. 2017) and described changes in the thalamic–precuneate system in disorders of consciousness (Soddu et al. 2010; Fernández-Espejo et al. 2012). Previous studies in macaques (Yeterian and Pandya 1985, 1988; Schmahmann and Pandya 1990; Leichnetz 2001)

have reported diffuse projections from nearly all regions of the thalamus to the precuneus, but these reports were generally based on a few cases and descriptions were largely qualitative. Here, we re-examined in more detail the thalamic afferents to the precuneate gyrus in macaques based on a set of localized retrograde tracer injections. These data add to a recent body of quantitative descriptions of the subcortical input to the caudomedial lobe (Buckwalter et al. 2008; Gamberini et al. 2016; Impieri et al. 2018) and allow us to look for specific functional trends within this large cortical region.

Materials and methods

Fluorescent tracers were injected in the precuneate cortex of four adult monkeys (*Macaca fascicularis*, 2.5–4.9 kg) (Fig. 1). Details of the location of injections and tracers used are presented in Table 1. Experimental protocols conformed to the guidelines of the Australian Code of Practice for the Care and Use of Animals for Scientific Purposes and the European Union Directive 86/609/EEC and the revised Directive 2010/63/EU. The Monash University Animal Experimentation Ethics Committee and the University of Bologna Bioethics Committee approved the experimental procedures (University of Bologna Permit No. 170/2015-PR, 19/03/2015; Monash University Permits No. MARP2012/082, SOBSA/P/2010/05, SOBSA/P/2010/28).

Surgical procedures

A detailed description of experimental procedures is available in a previous publication, which included data on cortical connections from many of the same animals (Passarelli et al. 2018). Surgeries were performed under aseptic conditions and full anesthesia, with the heart rate, blood pressure, respiratory depth, and body temperature monitored continuously. The protocol for anesthesia varied between animals, reflecting procedures approved by the two Universities as well as refinements introduced during the project. Animal A9 (injection cases 1 and 2; see Table 1) was pretreated with injections of atropine (0.04 mg/kg, i.m.) and ketamine hydrochloride (15 mg/kg, i.m.) and, after 30 min, anesthetized with sodium thiopental (8 mg/kg, i.v.), with additional doses administered as required. Animals MF3 and MF4 (injection cases 3, 5, 6, and 8) were pre-medicated with i.m. injections of diazepam (3.0 mg/kg) and atropine (0.2 mg/kg), and anesthetized 30 min later with alfaxalone (10 mg/kg, i.m.), with supplemental doses (5 mg/kg) administered i.v. as required. Finally, animal MF6 (injection cases 4 and 7) was pre-medicated with i.m. injections of diazepam (1.0 mg/kg) and atropine (0.04 mg/kg), and anesthetised 30 min later with an i.m. injection of ketamine (2 mg/kg), medetomidine (0.02 mg/kg), and butorphanol (0.1 mg/kg), after which the animal was intubated and maintained with isoflurane (0.5–2%). In all cases, hydration was provided by constant i.v. infusion of Hartmann's solution. Dexamethasone (0.3 mg/kg, i.m.) and Norocillin (25 mg/kg, i.m.) were also administered at the start of the procedures. The animals were placed in a stereotaxic frame and a craniotomy was performed over the posterior parietal cortex. To reach the mesial surface of the hemisphere, a portion of the posterior parietal cortex of the contralateral hemisphere (which likely included parts of areas PE, PEc, V6A and/or PGm) was retracted or removed by aspiration, the falx cerebri was retracted, and the mesial surface exposed. Injection sites were selected by direct visualization relative to the cingulate and parieto-occipital sulci. The fluorescent tracers were typically injected using a microsyringe that had a glass micropipette attached to its needle. In 2 cases (Table 1), the retrograde fluorescent tracers Fast blue (FB) and Diamidino Yellow (DY) were directly applied into the cortex as crystals (approximately 100–200 µm in diameter), with the aid of blunt tungsten wires (Rosa et al. 2005). Analgesics (ketorolac, 1 mg/kg, i.m., Temgesic, 0.01 mg/kg, i.m., or Carprofen, 4–5 mg/kg, s.c.) were provided postoperatively.

The day after the surgery, the animals had some difficulty in performing reaching and grasping movements with the hand contralateral to the lesion (for example, to get a piece of fruit) and were somewhat slow in putting the opposite foot on the ground; eating and drinking behavior were as before surgery and the animals did not look in pain or otherwise distressed. Impairments are overall in agreement with the functional properties of the lesioned areas (Battaglini et al. 2002; Fattori et al. 2017; Gamberini et al. 2018). The motor-related symptoms disappeared a few days after surgery.

Tissue processing

After a survival period of 14 days, the animals were anesthetized (as above, for different cases) and administered a lethal i.v. barbiturate injection. They were then perfused with several litres of heparinised saline, followed by 4% paraformaldehyde in 0.1 M phosphate buffer at pH 7.4 (followed by 5% buffered glycerol in animal A9). The brains were cryoprotected by immersion in graded series of buffered sucrose (10–30%, most animals) or glycerol (10–20%, animal A9). Coronal sections (50 µm in most cases and 60 µm in A9) were obtained using a freezing microtome. One in five sections was left unstained for observation under a fluorescence microscope. Adjacent sections were stained for Nissl substance, myelin (Gallyas 1979), and cytochrome oxidase (Wong-Riley 1979), and a fifth series was left in reserve.

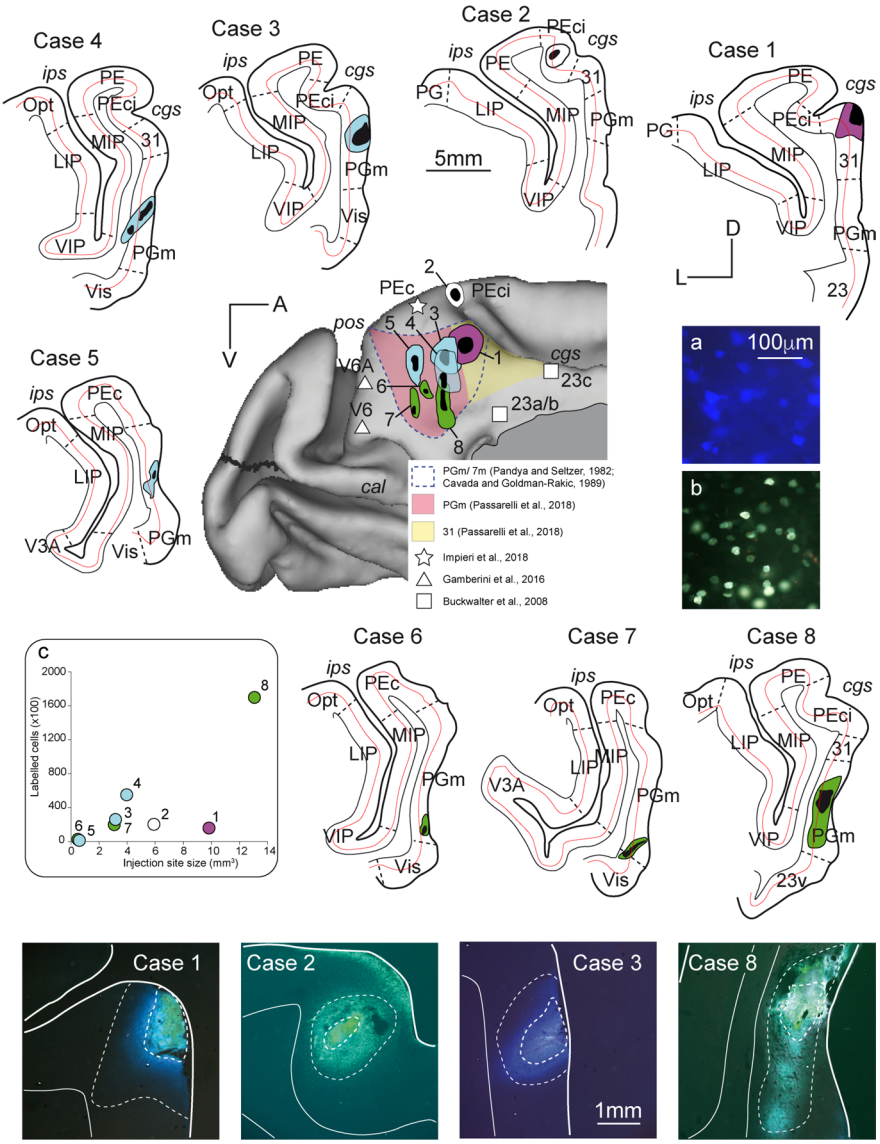

Fig. 1 Summary of injection site locations. Top: medial view of a reconstruction of a macaque left hemisphere showing the location of the injection sites, based on computerized registration of the brains of the different animals relative to the sulcal pattern. Injections in areas 31 (purple), PEci (white), the dorsorostral part of area PGm (cyan), and the ventrocaudal part of area PGm (green) are indicated. The dashed lines indicate the approximate extent of area PGm according to previous studies (Pandya and Seltzer 1982; Cavada and Goldman-Rakic 1989a, b; Morecraft et al. 2004). The pink and yellow shading indicates the revised borders of areas PGm and 31 (Passarelli et al. 2018). White symbols indicate the approximate locations of injection sites in neighbouring areas according to other studies: star, injections in PEc (Impieri et al. 2018); triangles, injections in V6 and V6A (Gamberini et al. 2016); squares, injections in subdivisions of 23 (Buckwalter et al. 2008). For each injection, the core (dark spot) and the halo zone (coloured region around the core) are shown. Dashed lines indicate the average architectonic border of injected (PGm, 31 and PEci) and neighbouring areas. The location of the injection sites in the cortical thickness is shown on single coronal sections. Red lines depict traces of layer 4 and correspond to the boundary between superficial and deep layers. Bottom: epifluorescent photographs of coronal sections through the injection sites in 4 cases. Case 1: FB injection of area 31, Case 2: DY injection of area PEci, Case 3: FB injection of the dorsorostral area PGm, Case 8: DY injection of the ventrocaudal area PGm. Scale bar = 1.0 mm. Insets **a** and **b** show examples of FB- and DY-labelled cells (from cases 1 and 2, respectively) in greater magnification. Inset **c**: the scatter plot shows that the size of the injection site (in mm^3) is related to the number of labelled cells in the cortex and thalamus. *cal* calcarine sulcus, *cgs* cingulate sulcus, *ips* intraparietal sulcus, *pos* parieto-occipital sulcus, *D* dorsal, *L* lateral, *V* ventral, *A* anterior

All sections were coverslipped with DPX mounting medium after rapid dehydration in ethanol and clearing with xylene.

Data analysis

The unstained sections of the hemispheres ipsilateral to

Table 1 Injection sites and neuronal tracers employed in the experiments

Case	Animal hemisphere[a]	Injected area	Tracer[b]	Amount and concentration of tracer	Number of cortical[c]/thalamic labelled cells
1	A9-R	31	FB	0.2 µl, 1%	15,581/332
2	A9-R	PEci	DY	1 crystal	19,949/386
3	MF3-R	Dorsorostral PGm	FB	1 crystal	25,535/453
4	MF6-L	Dorsorostral PGm	FB	0.35 µl, 1.5%	53,398/1742
5	MF3-R	Dorsorostral PGm	FR	0.25 µl, 15%	1281/92
6	MF4-R	Ventrocaudal PGm	FR	0.4 µl, 15%	2496/92
7	MF6-L	Ventrocaudal PGm	DY	0.35 µl, 1.5%	19,674/150
8	MF4-R	Ventrocaudal PGm	DY	1 µl, 1.5%	166,982/2906

[a]R right; L left

[b]Tracer abbreviations: *FB* Fast Blue, Polysciences Europe; *DY* Diamidino Yellow, Sigma-Aldrich; *FR* Fluoro Ruby, Invitrogen–Molecular Probe

[c]Extrinsic ipsilateral connections

the injection sites were scanned for labelled neurons with microscopes under fluorescence illumination (Zeiss Axioscope 2 Plus). For all sections examined, the outer and inner boundaries of the cerebral cortex, the outlines of the injection sites, and the location of labelled cells were mapped at 500–600 µm intervals (1 in 10 sections) using a digitizing system attached to the microscopes (MD3 digitizer and MDPlot software, Accustage). MDplot drawings were aligned with the nearest histological sections to assign labelled neurons to thalamic nuclei. The average extent of PGm and locations of injection sites are reported on a reference 3D reconstruction of a macaque brain from the computerized registration of different brains, using the CARET software (https://www.nitrc.org/projects/caret/; Van Essen et al. 2001), as described previously (Gamberini et al. 2009; Passarelli et al. 2018).

Assignment of injection sites to cortical areas PGm, PEci, and 31 was based on previously described cyto- and myeloarchitectural features (Fig. 2; Pandya and Seltzer 1982; Morecraft et al. 2004; Passarelli et al. 2018). Identification of the thalamic nuclei (Fig. 2) was based on the atlas of Olszewski (1952) and more recent refinements summarized in Mai and Forutan (2012). For identification of the pulvinar subdivisions and the lateral posterior nucleus, which contained the bulk of labelled cells in our study, the descriptions by Schmahmann and Pandya (1990) and Romanski et al. (1997) were useful. Thus, in the rostral pole of the pulvinar, the oral subdivision is characterized by a low cell density. Caudally, the medial and lateral subdivisions are typically present at the same levels; the medial subdivision can be distinguished by a comparatively high cell density and the lateral pulvinar by the numerous fibre bands crossing through it. The lateral posterior nucleus occupies a dorsal and lateral position relative to the medial pulvinar, and can be identified by its moderate-sized cells and darker staining. We noted small variations in the boundaries of the different thalamic nuclei across hemispheres, as reported before (Schmahmann and Pandya 1990). Table 2 outlines the terminology followed in the present work.

Because the number of labelled neurons depends on many factors, including the type and volume of the injected tracer (e.g., results of our statistical analysis in the following section), and the laminar placement of the injection sites (Jones 2001), the distribution of labelling in each nucleus was expressed as a fraction of the total number of recorded neurons in thalamus, case by case, as reported in the previous papers (Buckwalter et al. 2008; Gamberini et al. 2016).

Results

We describe the thalamic afferents to the macaque precuneate cortex after 8 retrograde tracer injections. As shown in Fig. 1, areas 31 and PEci each received one injection, and area PGm 6 injections. Three of the PGm injections were placed in the dorsorostral part of this area (cases 3–5), and 3 in the ventrocaudal part (cases 6–8), defined according to our recent study (Passarelli et al. 2018). As detailed in this study, the ventrocaudal part of PGm (which has not been sampled in earlier studies) differs from the dorsorostral part in terms of cortico-cortical connections.

The number of labelled neurons in the cortex and thalamus varied between cases (Table 1), likely reflecting both differences in tracer sensitivity and in the extent of injections (Fig. 1); in particular, our analysis showed that the number of observed labelled cells is related to the size of the injection site (Fig. 1, inset c; Pearson's $r = 0.757$, $p < 0.05$). In agreement with previous reports on the thalamocortical connectivity of posterior parietal areas (Gamberini et al. 2016; Impieri et al. 2018), the number

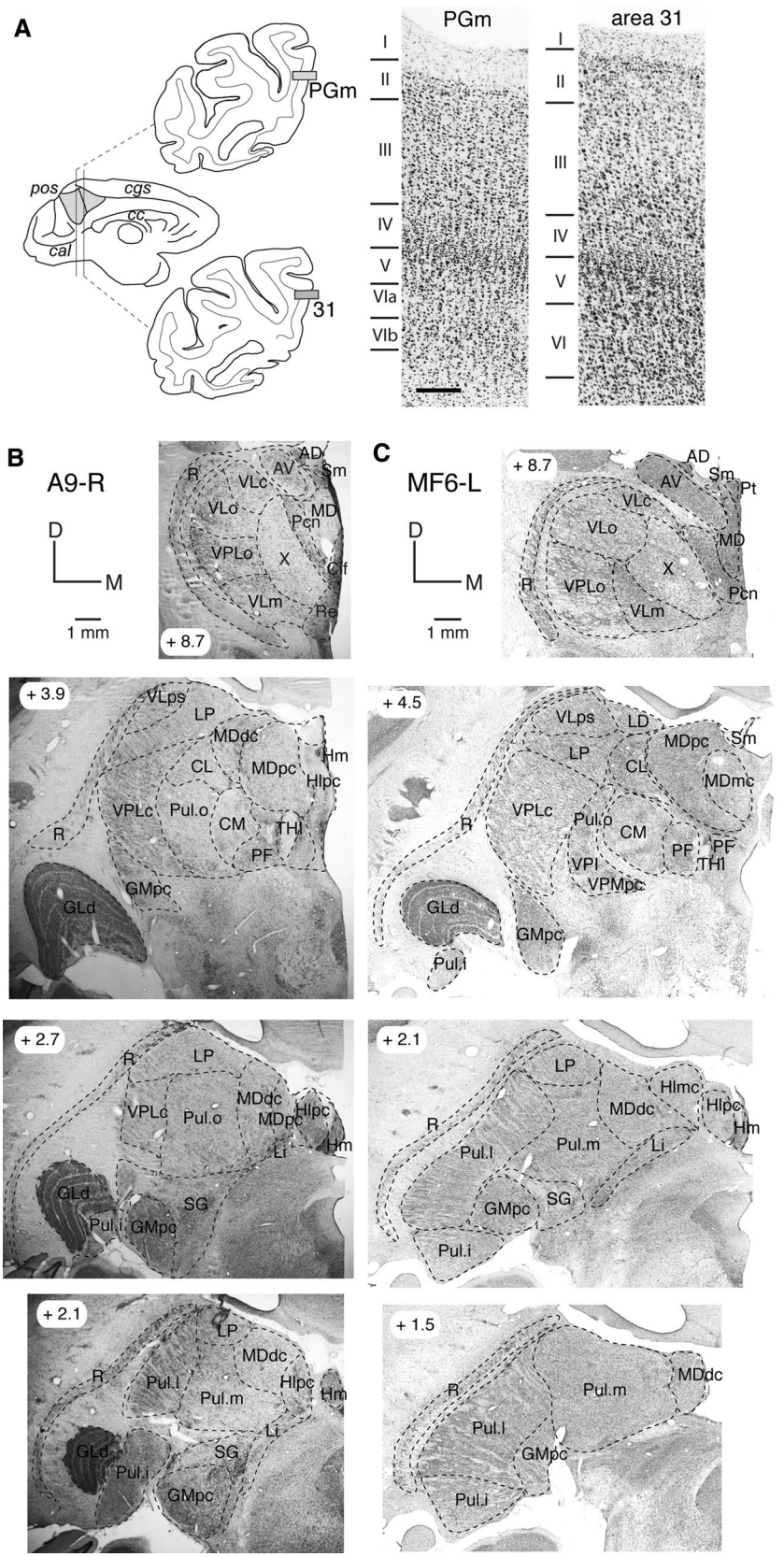

Fig. 2 Cytoarchitecture of injected areas and of thalamic nuclei. **a** Low-power photomicrographs showing the cytoarchitectural criteria used to distinguish areas in the precuneus cortex. Coronal sections were taken at the levels indicated on the inset. Scale bar = 200 µm. **b**, **c** Low-power photomicrographs of representative coronal sections from animals A9-R (**b**) and MF6-L (**c**) showing the cytoarchitectonic subdivisions of thalamic nuclei. Scale bar = 1 mm. *cc* corpus callosum, *M* medial. For the nomenclature of thalamic nuclei, see the list of abbreviations

Table 2 Correspondence of nomenclature of the thalamic nuclei involved in this study

Thalamic regions (Mai and Forutan 2012)	Olszewski (1952)	Present study
Anterior (or superior)	AD	AD
	AV	AV
	AM	AM
	LD	LD
Medial	MD	MD
	MDmc	MD
	MDpc	MD
	MDmf	MD
	MDdc	MD
Lateral (motor)	VA	VA
	VAdc	VA
	VAmc	VA
	VApc	VA
	VApc/dc	VA
	VLo	VA
	VLc	VL
	VLps	VL
	VLm	VL
	X	VL
	VPLo	VL
Lateral (sensory)	VPLc	VPL
	VPM	VPM
	VPMpc	VPM
	VPI	VPI
Intralaminar	Cn. Md	CM
	Pf	PF
	Csl	Csl
	Pcn	Pcn
	Cl	CL
	SG	SG
	Li	Li
Periventricular	Re	Re
	Pt	Pt
	Pa	Pa
	Clc	Clc
	Cdc	Cdc
	Cif	Cif
	Cs	Cs
Posterior	LP	LP
	Pul.o	Pul.o
	Pul.m	Pul.m
	Pul.l	Pul.l
	Pul.i	Pul.i
	GLd	GLd
	GMmc	GMmc
	GMpc	GMpc

of labelled neurons in the thalamus represented a small fraction of the extrinsic (ipsilateral cortical and thalamic) afferents to each area of the precuneate cortex (area PEci: 1.9%; area 31: 2.1%; dorsorostral PGm: $2.8 \pm 2.6\%$; ventrocaudal PGm: $1.6 \pm 1.4\%$).

Areas PGm, 31, and PEci all received substantial input from the associative nuclei of the posterior thalamus and moderate inputs from medial and lateral regions (Mai and Forutan 2012). Nevertheless, each of the studied areas could be distinguished on the basis of receiving unique connectivity patterns from specific nuclei, as well as the spatial arrangement of labelled cells, as described in the following sections.

Thalamic afferents to areas PEci and 31

Figure 3 illustrates the distribution of labelled cells in the thalamus after injections in areas 31 and PEci in animal A9 (cases 1 and 2, respectively). Results from these injections were similar, with labelled cells mainly concentrated in dorsal portions of the central-posterior thalamus, although differences in their spatial distribution were often observed within the labelled nuclei (see Fig. 3d–g). The proportions of labelled cells in the various nuclei are reported in Table 3. The majority of projecting cells were located in the pulvinar complex, in particular in the oral subdivision (Pul.o), and the lateral posterior nucleus (LP). Afferents from the posterior thalamic nuclei accounted for > 50% of the total thalamic input in both cases. Projection cells in LP were found mainly in the ventral half of the nucleus, with cells labelled by the area 31 injection occupying a dorsomedial location relative to those labelled by the PEci injection (Fig. 3d–g). Moderate afferents to both areas arrived from the mediodorsal nucleus (Fig. 3c–g), the ventrolateral nucleus (mainly from the postrema part, VLps, Fig. 3d, e), and the intralaminar region (in particular, the anterior nucleus CL, Fig. 3e). Despite these shared afferents, areas 31 and PEci could also be distinguished by differential input. Thus, the PEci injection labelled many cells in the somatosensory thalamus (ventral posterior lateral nucleus, caudal part, VPLc, Fig. 3d–g; VPL in Table 3), while only sparse cells were found after the area 31 injection. Conversely, the injection in area 31 revealed overall stronger afferents from the intralaminar region (~ 14% of total thalamic projections, Table 3) with the inclusion of small projections from the paracentral (Pcn) and suprageniculate (SG) nuclei and additional minor afferents from the anterior (AV) and periventricular (Re, Cdc, Cif) nuclei (Fig. 3a, b), as well as from the ventral anterior (VA) nucleus and the anterior (VLo) and medial (VLm) subdivisions of the ventral lateral nucleus (Fig. 3a, VL in Table 3).

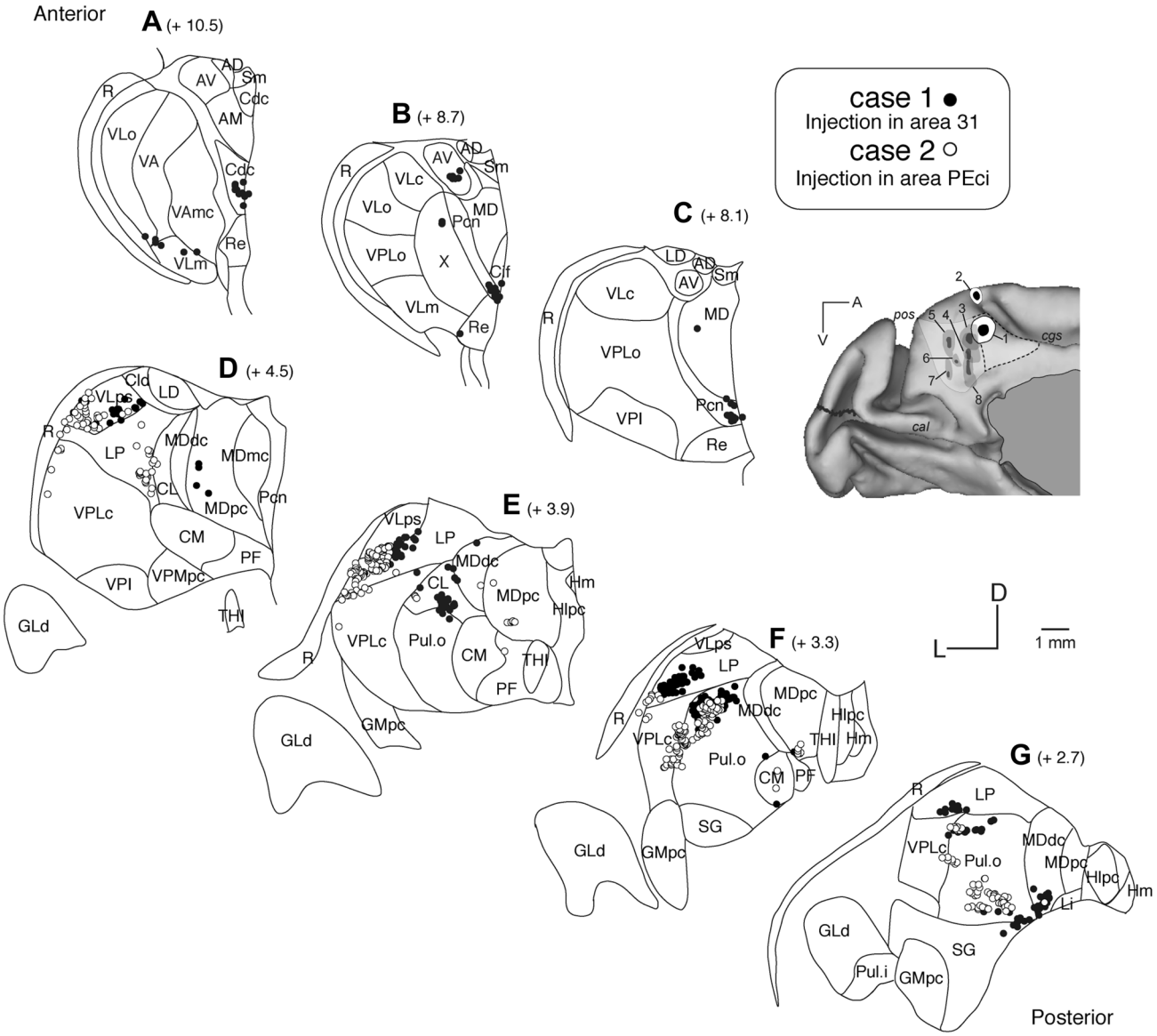

Fig. 3 Thalamic afferents to areas 31 and PEci. Seven coronal sections (**a**–**g**) through the thalamus illustrating the distribution of labelled cells after injections in areas 31 (case 1, black circles) and PEci (case 2, white circles). In the top right of the figure, a medial view of a reconstruction of a macaque left hemisphere showing the location of the injection sites (shown here and in Figs. 3, 4, and 5). The numbers in parentheses, shown here and in Figs. 4, 5, and 6, correlate to the approximate coronal level reported by Olszewski (1952). For the nomenclature of thalamic nuclei, see the list of abbreviations

Thalamic afferents to area PGm

Figures 4, 5, 6 show the distribution of thalamic labelling in cases with injections in dorsorostral (Fig. 4, case 4; Fig. 5, cases 3 and 5) and ventrocaudal (Fig. 4, case 7; Fig. 6, cases 6 and 8) parts of PGm. All 6 injections in PGm resulted in similar patterns of labelling in the thalamus, with some variation in the relative density and the origin of projections depending on the location of injection sites (see Table 3 for quantitative analysis).

Similar to the injections in areas 31 and PEci, the LP and the pulvinar complex nuclei contributed the bulk of projections to PGm. Injections in PGm revealed labelled neurons across the medial, lateral, and oral subdivisions of the pulvinar (Pul.m, Pul.l, and Pul.o, respectively). However, the numbers of labelled cells in the Pul.o were much lower (on average, < 4%) compared to those in the area 31 and PEci cases (> 30%). Afferents from the medial pulvinar were numerous (15–31% across cases), and afferents from the lateral division were variable (0.5–33%) and

Table 3 Summary of the projections in thalamic nuclei after injections in areas 31, PEci, and PGm

Injected area	Area 31	PEci	Dorsorostral PGm			Ventrocaudal PGm		
Case	1	2	3	4	5	6	7	8
Thalamic regions								
Anterior								
AD	–	–	–	–	–	–	–	*
AV	2.1	–	–	0.7	–	2.2	0.7	0.8
AM	–	–	–	0.9	–	–	1.3	*
LD	–	–	0.9	7.2	2.2	–	20.7	2.3
Total	**2.1**	**0.0**	**0.9**	**8.8**	**2.2**	**2.2**	**22.7**	**3.1**
Medial								
MD	12.0	3.6	11.3	14.6	1.1	3.3	12.7	2.3
Total	**12.0**	**3.6**	**11.3**	**14.6**	**1.1**	**3.3**	**12.7**	**2.3**
Lateral								
VA	1.2	–	1.8	0.9	–	4.3	–	3.5
VL	7.2	7.3	7.7	6.8	6.5	23.9	12.0	5.6
VPL	*	8.8	–	*	–	–	–	–
Total	**8.4**	**16.1**	**9.5**	**7.7**	**6.5**	**28.2**	**12.0**	**9.1**
Intralaminar								
CM/PF	*	0.8	6.8	2.7	–	2.2	–	*
Csl	–	–	–	*	1.1	–	0.7	*
Pcn	6.3	–	4.0	6.8	–	–	2.0	*
CL	6.6	1.8	2.0	1.0	2.2	–	–	0.6
SG	1.5	–	*	*	–	–	–	*
Li	–	–	3.5	1.0	2.2	1.1	–	1.0
Total	**14.4**	**2.6**	**16.3**	**11.5**	**5.5**	**3.3**	**2.7**	**1.6**
Periventricular								
Re	*	–	–	–	–	2.2	–	–
Clc	–	–	–	–	–	4.3	–	*
Cdc	3.0	–	1.6	3.4	–	1.1	1.3	–
Cif	*	–	–	–	–	–	–	–
Total	**3.0**	**0.0**	**1.6**	**3.4**	**0.0**	**7.6**	**1.3**	*****
Posterior								
LP	28.3	36.8	21.8	31.6	30.4	16.3	32.0	27.2
Pul.o	30.4	40.9	5.5	3.6	4.3	6.5	1.3	1.0
Pul.m	–	–	25.2	16.8	17.4	23.9	15.3	31.0
Pul.l	–	–	7.5	0.5	32.6	8.7	–	24.0
Total	**58.7**	**77.7**	**60.0**	**52.5**	**84.7**	**55.4**	**48.6**	**83.2**
Other			*	*				
Thalamus total	**100.0**	**100.0**	**100.0**	**100.0**	**100.0**	**100.0**	**100.0**	**100.0**

Relative percentages of labelled cells are listed for each nucleus and for each group of nuclei (in bold)

Dash represents no observed labelling. * < 0.5% of total projections

were not detected in injection case 7 (Figs. 4f, 5e, f, 6f; Table 3).

Consistent labelling, albeit consisting of smaller numbers of labelled cells, was found in the mediodorsal (MD) nucleus (1–15%) and the ventrolateral nuclei (6–24%, VLc, VLps in Figs. 4, 5, 6). In some cases, afferents originated in the lateral motor VA nucleus; these were somewhat emphasized in two of the cases with ventrocaudal injections (~4%, cases 6 and 8, Table 3). In the anterior region of the thalamus, labelling of variable strength was present in the laterodorsal (LD) nucleus in 5 out of 6 cases. This label was particularly strong (~21%) in case 7 with injection in ventrocaudal PGm. The other nuclei of the anterior complex (AV, AM, and AD) contained a few additional labelled cells. Afferents from the intralaminar nuclei (CM/PF, Pcn, Csl, CL, SG, and Li) were also present in several cases (Table 3); these tended

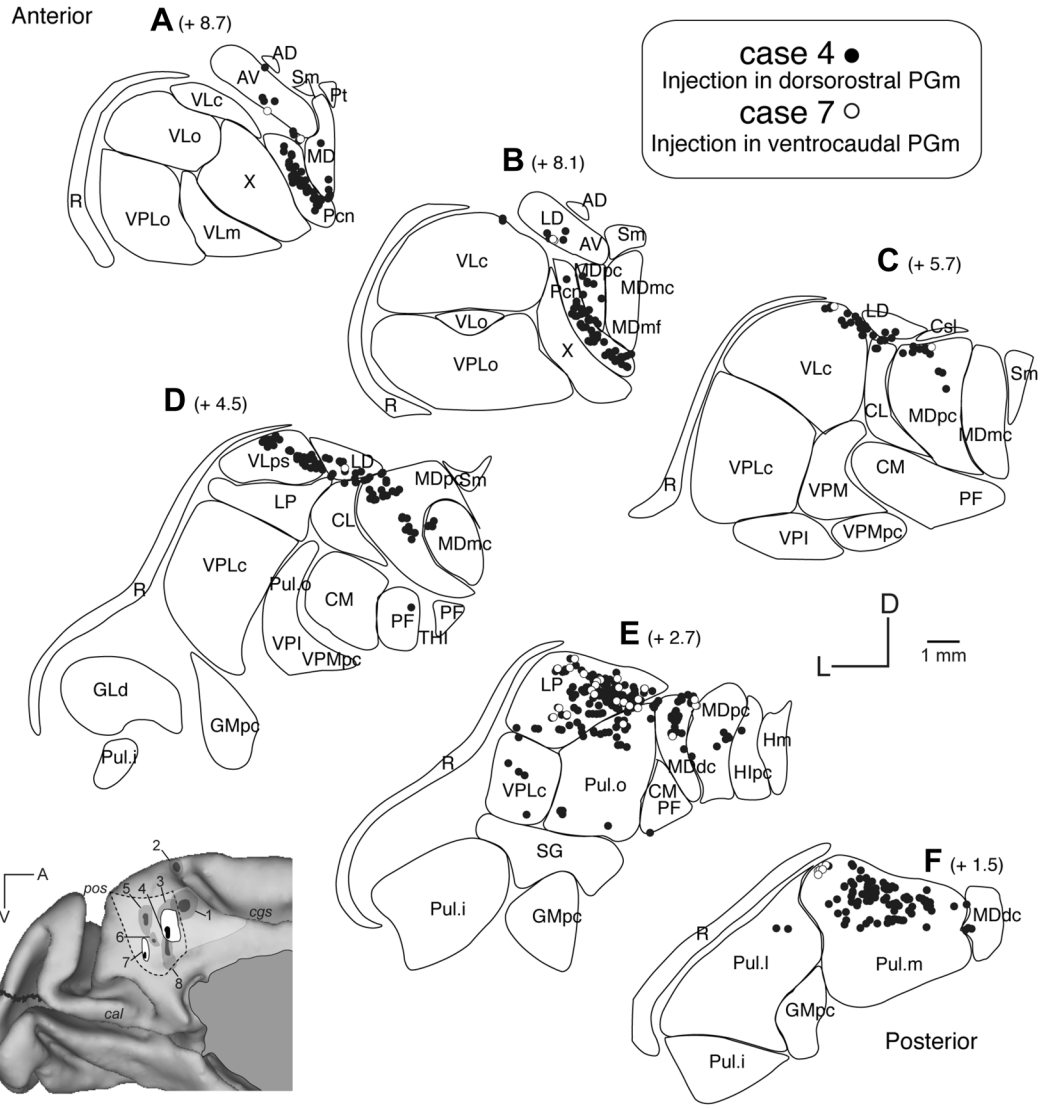

Fig. 4 Thalamic afferents to dorsorostral and ventrocaudal sector of PGm. Six coronal sections from cases 4 and 7 are reported. Black circles represent the labelled cells after injection in the dorsorostral sector of PGm (case 4), and white circles after injection in the ventrocaudal sector of PGm (case 7) in the same hemisphere. For the nomenclature of thalamic nuclei, see the list of abbreviations. Other details and abbreviations as in Figs. 1 and 3

to be stronger after injections in the dorsorostral part of PGm (on average ~ 11% in cases 3–5). Finally, the periventricular region contained overall the lowest numbers of labelled cells, with the exception of case 6 with moderate numbers (7.6%), especially in the central latocellular nucleus (Clc).

General trends in thalamic afferents to the precuneus

Taken together, our results, based on multiple injections in the precuneus and quantitative analyses, indicate that areas PGm, 31 and PEci receive their main input from the posterior thalamus, in different combinations from the lateral posterior and the pulvinar complex, and moderate input from the medial, lateral, and intralaminar regions. This information is summarized in Fig. 7. Three main features of the pattern of thalamic input to the precuneus are evident in our data. First, results highlight differential roles for PGm (with strong connectivity with the associative medial and the visual lateral divisions of the pulvinar), and areas 31 and PEci (which receive afferents from the oral division). Second, our injections hint at some degree of topographical organization in the projections from LP and the medial pulvinar, such that more dorsal parts of these nuclei send projections to ventral parts of the precuneus (ventrocaudal PGm: Fig. 6d–f). Conversely, locations in the dorsal precuneus are targeted by central/ventral parts of LP (PEci/31: Fig. 3d–g, dorsorostral PGm: Fig. 5d) and the medial pulvinar (dorsorostral

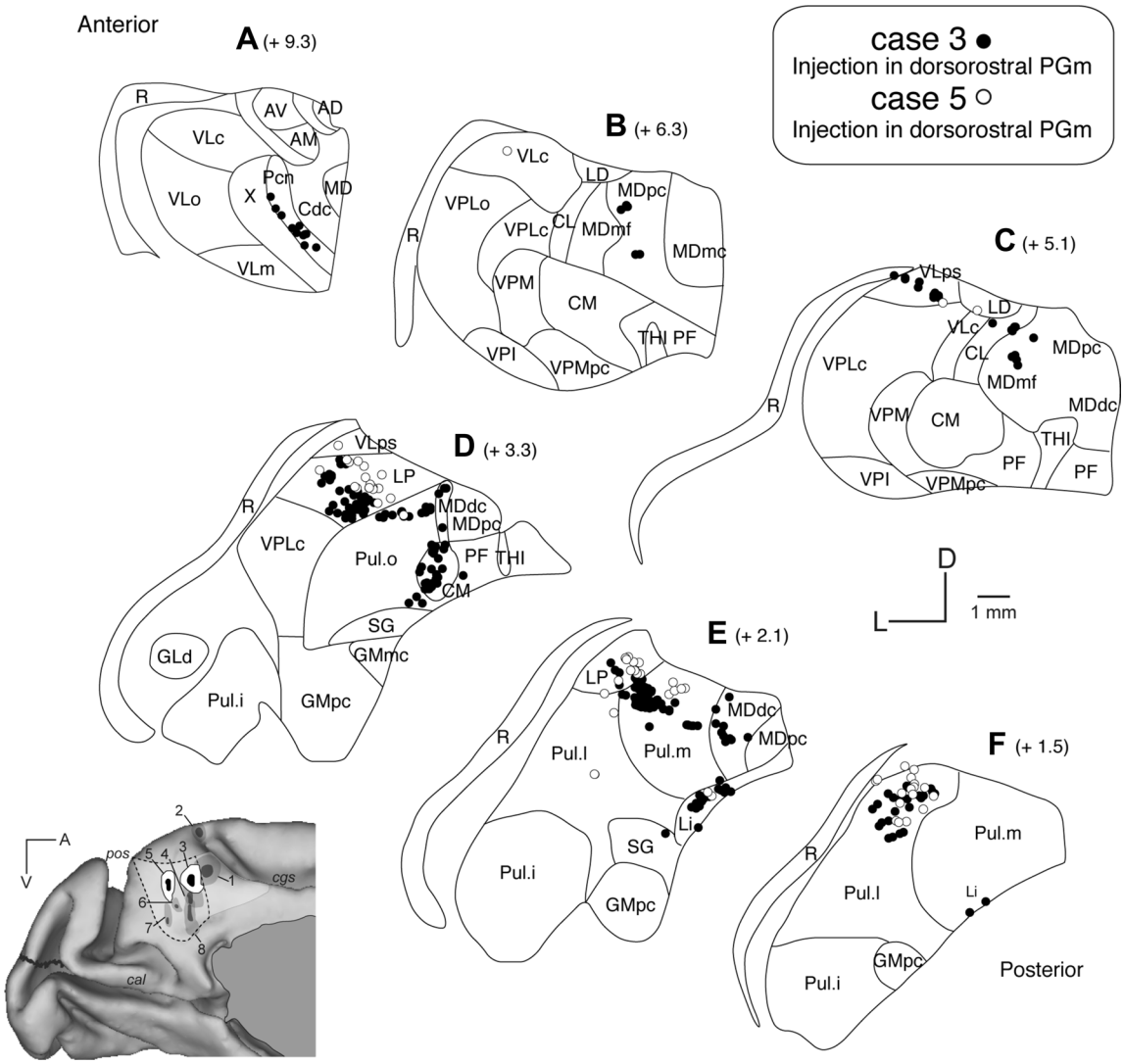

Fig. 5 Thalamic afferents to dorsorostral sector of area PGm. Six coronal sections from cases 3 (black circles) and 5 (white circles) are reported. For the nomenclature of thalamic nuclei, see the list of abbreviations. Other details and abbreviations as in Figs. 1 and 3

PGm: Fig. 5e). A third feature relates to the lateral group of thalamic nuclei, which contained consistent labelling after injections in all three areas. Mai and Forutan (2012) proposed the subdivision of the lateral region into a "motor" and "sensory" domain based on relevant functional properties. In line with this proposal, areas PGm and 31 showed modest labelling (< 10% of total labelled cells) in the "motor" thalamus, including the VA and VL nuclei, while numbers of labelled cells after injection in area PEci were balanced in the "sensory" (VPL) and "motor" domain (approximately 8% in each).

Comparison of precuneate cortex with neighbouring areas

In the final part of our analysis, we compare the thalamic afferents to areas PGm, 31, and PEci with those to neighbouring cortical areas (Fig. 1) using published quantitative data sets. Our analysis included extrastriate area V6, posterior parietal areas V6A (Gamberini et al. 2016) and PEc (Impieri et al. 2018), and subdivisions of area 23 (Buckwalter et al. 2008). Figure 8 presents a graphic overview of the patterns of thalamic projections to the caudal medial lobe. On the basis of connections with the posterior thalamus, it is possible to identify two main patterns of connectivity oriented as oblique bands, with each of the areas forming the caudomedial lobe retaining distinct connectional features.

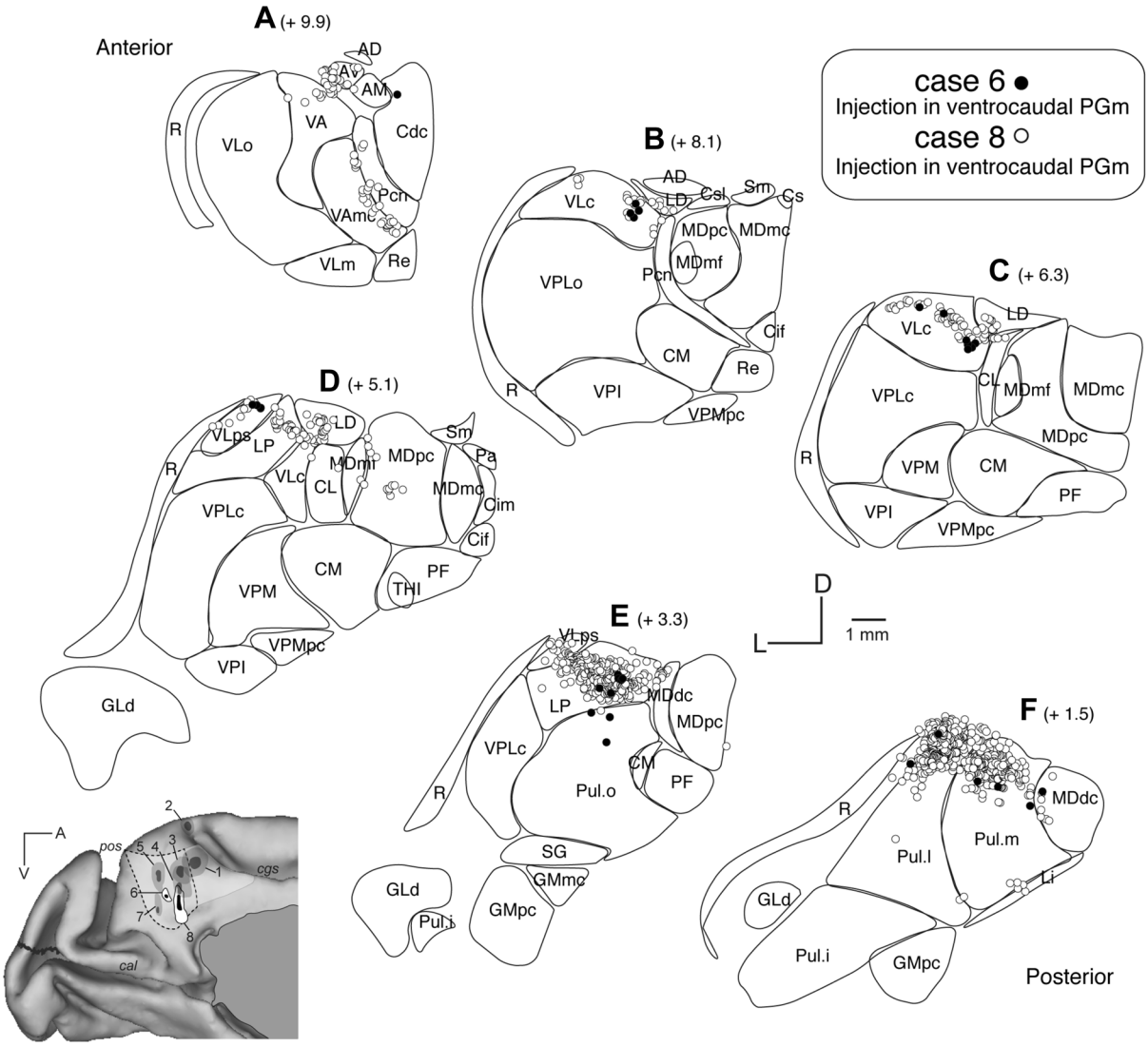

Fig. 6 Thalamic afferents to ventrocaudal sector of area PGm. Six coronal sections from cases 6 (black circles) and 8 (white circles) are reported. For the nomenclature of thalamic nuclei, see the list of abbreviations. Other details and abbreviations as in Figs. 1 and 3

A "posterior" connectional pattern is evident for areas V6A, PEc, and PGm. This group shares strong projections from the posterior thalamus with an emphasis on projections from the medial pulvinar. Projections from the lateral posterior nucleus become progressively weaker in a rostral direction (in areas PEc and PGm). Additional common projections arrive from the lateral and intralaminar thalamus, but these are generally moderate/weak. An "anterior" pattern consists of the posterior cingulate areas (PEci, 31, 23c). Input from the posterior thalamus is still dense, but, different to the posterior parietal pattern, projections from the oral pulvinar become evident, emphasizing an associative skeletomotor role.

Finally, two ventral areas, V6 and 23a/b, are at the limits of these patterns. Area V6 in the ventral–caudal part of the medial lobe is unique in its emphasis on the visual modality with inputs from the lateral and inferior subdivisions of the pulvinar and the lateral geniculate (Gamberini et al. 2016). A second strong contingent of afferents to V6 is noted from the intralaminar (Pcn) and periventricular (Cdc) region; input from the lateral posterior, mediodorsal, and the ventral region, typical for posterior parietal areas, is still present but in much lower percentages. Area 23a/b, in the ventrorostral pole of the caudal medial cortex, shows the strongest input from the intralaminar nuclei, followed by inputs from the anterior region, the mediodorsal nucleus, and the medial subdivision of pulvinar.

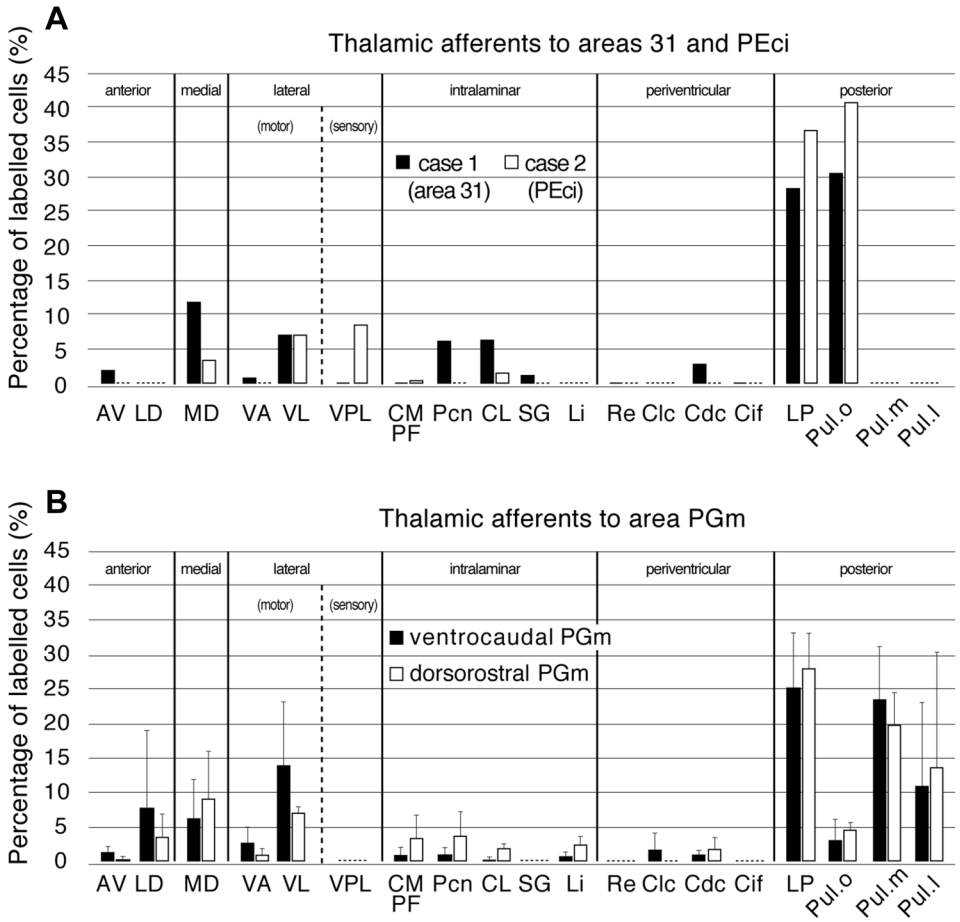

Fig. 7 Summary of the thalamic afferents after injections in precuneate cortex. **a** Thalamic afferents to areas 31 and PEci in cases 1 and 2, respectively. **b** Average percentages of labelled cells in thalamic nuclei after tracer injections in dorsorostral and ventrocaudal sectors of area PGm. Vertical bar, SD. Dashed lines represent nuclei where thalamic label was not observed. Gross subdivisions of the thalamus into six regions follow the proposal by Mai and Forutan (2012). For the nomenclature of thalamic nuclei, see list of abbreviations and Table 2.

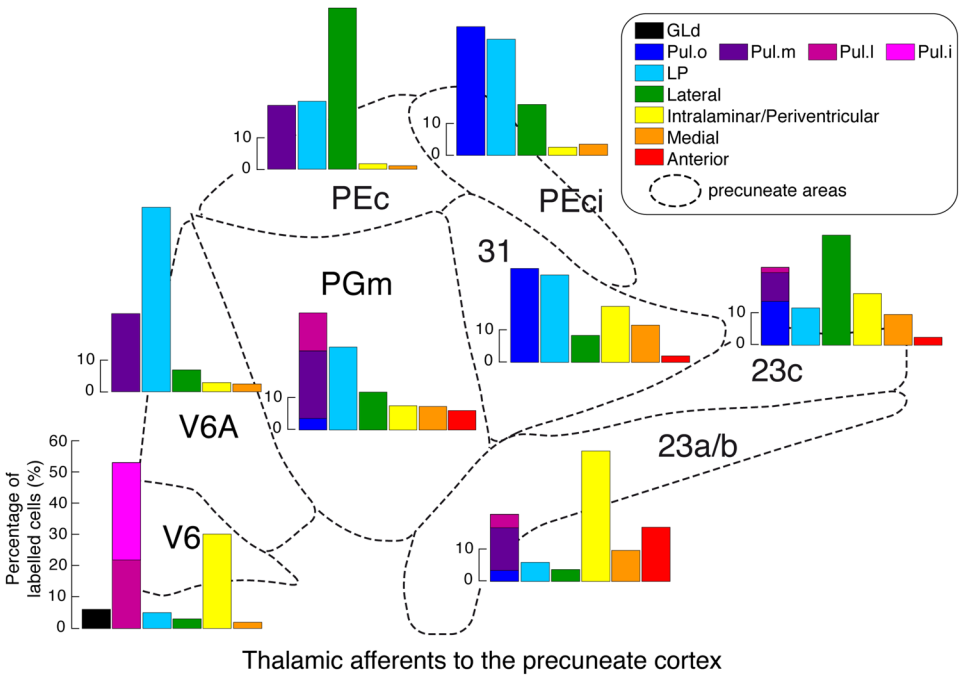

Fig. 8 Patterns of thalamic input to precuneus and neighbouring areas. The "posterior" pattern of connections includes areas V6A (population data from Gamberini et al. 2016), PEc (population data from Impieri et al. 2018), and PGm (population data from present study); the "anterior" pattern including areas PEci (case 2 of present study), 31 (case 1 of present study) and 23c (case 4 of Buckwalter et al. 2008). For comparison, thalamic afferents after injections in areas V6 (population data from Gamberini et al. 2016) and 23a/b (case 1 of Buckwalter et al. 2008) are represented. For the nomenclature of thalamic nuclei, see list of abbreviations and Table 2

Discussion

The main conclusion of this tracing study is that the macaque area PGm, defined histologically, integrates information from a set of visual, association, motor, and limbic regions of the thalamus. The general lack of input from thalamic structures associated with somatomotor functions (such as the ventral posterior complex and the oral pulvinar; Grieve et al. 2000; Padberg et al. 2009) differentiates PGm from the adjacent superior parietal areas, including PEci and 31, specialized in analyses related to the use of the limbs.

The projections from multiple thalamic regions parallel the rich cortical connectivity of PGm with visual, parietal association, dorsolateral prefrontal, and limbic systems (Pandya and Seltzer 1982; Cavada and Goldman-Rakic 1989a, b; Leichnetz 2001; Passarelli et al. 2018). Our earlier study on the cortical connectivity of the area (Passarelli et al. 2018) showed evidence of anatomical heterogeneity: pathways from premotor cortex preferentially targeted dorsorostral PGm, whereas ventrocaudal PGm received preferential connections from extrastriate and posterior cingulate/retrosplenial areas. Similar trends were not obvious in the organization of thalamocortical projections (Table 3; Fig. 7): dorsorostral PGm showed somewhat denser input from the intralaminar region, whereas ventrocaudal PGm received stronger projections from the lateral motor (VL/VA) and anterior limbic nuclei (mainly LD and AV), but differences were generally subtle. In this regard, previous findings rather support our observation here that the pattern of subcortical connectivity is often a relatively poor predictor of architectonic variation and/or regional specialization (Boussaoud et al. 1992; Buckwalter et al. 2008; Gamberini et al. 2016). We did, however, observe variability in some of the thalamic projections to PGm; for example, projections from the limbic lateral dorsal nucleus, the ventral lateral nucleus, and the lateral pulvinar targeted strongly specific parts of PGm (Table 3), hinting at a complex pattern of organization that cannot be fully captured by traditional notions of homogeneous cortical and thalamic connections throughout the borders of this architectural field (Passarelli et al. 2018).

Origins of major thalamic afferents to area PGm

The connections of PGm with the thalamus have been previously studied in macaques using anterograde and retrograde tracer injections in the cortex (Schmahmann and Pandya 1990; Leichnetz 2001; Parvizi et al. 2006; Buckwalter et al. 2008), but those studies generally targeted dorsal portions of this cytoarchitectural area, and robust quantitative data were reported only in one paper (Buckwalter et al. 2008). Despite differences in the type of tracers (retrograde or anterograde) or concentrations of fluorescent tracers (e.g., 3–4% for FB and DY in Buckwalter et al. 2008), present and earlier quantitative analyses converge in showing that the most substantial thalamic input to PGm (on average ~ 60% of total thalamic input) originates in the lateral posterior nucleus and the pulvinar. While most studies include projections from the oral, lateral, and medial divisions of the pulvinar, the large, bi-directional tracing study by Leichnetz (2001) only reported connections with the lateral and medial divisions.

The pulvinar complex and the lateral posterior nucleus constitute the numerically predominant projections of the thalamus to the parietal lobe (present findings; Cappe et al. 2007; Gamberini et al. 2016; Impieri et al. 2018; Schmahmann and Pandya 1990), and thalamic connections likely reflect parietal specializations in cognition and in the planning and control of motor actions (Battaglia-Mayer et al. 2001; Andersen et al. 2014; Hadjidimitrakis et al. 2015, 2019; Galletti and Fattori 2018). The LP, as an associative nucleus, provides information on somatic and attentional stimuli useful in the control of movements (Kamishina et al. 2008, 2009; Gamberini et al. 2016). A modulatory effect on these functions could be attained via the rich dopamine innervation of the monkey and human LP (García-Cabezas et al. 2007). The border between the LP and the pulvinar nuclei has been difficult to establish in neurophysiological studies (Acuña et al. 1986, 1990; Cudeiro et al. 1989), and the two are often considered as a functional unit. The medial pulvinar, much like LP, is viewed as a multimodal associative nucleus: it has extensive connectivity with high-order cortical systems (but not with early sensory areas, Homman-Ludiye and Bourne, 2019), it forms the subcortical component of the attentional network of the brain (Shipp 2003; Saalmann et al. 2012) and is involved in visuospatial processing and reward-based decision-making (Grieve et al. 2000; Wilke et al. 2013).

In addition to the strong input from the medial division, consistent (and, occasionally, of comparable strength) input to PGm was observed from the lateral pulvinar (on average ~ 10% of total, Table 3), which has connections with extrastriate and ventral stream areas (Gamberini et al. 2016; Kaas and Lyon 2007). Projection neurons to PGm were restricted to the dorsal part of this division, similar to what has been reported for the inferior parietal areas (Baleydier and Morel 1992; Hardy and Lynch 1992). This territory overlaps at least partially the field P4, which forms connections with peripheral representations of V2 and V4 (Ungerleider et al. 2014; Gattass et al. 2014). The same dorsal territory of the lateral pulvinar could also be coextensive with the field Pdm (Petersen et al. 1985) where neurons show poor retinotopic organization, but responses are enhanced for stimuli that become the focus of the animal's attention.

Minor thalamic afferents to area PGm

Secondary afferents to PGm arrived from several other thalamic nuclei, notably the VL and VA nuclei (on average, ~ 12% of total), the MD nucleus, and the anterior (superior) and intralaminar nuclei (~ 7% of total projections from each thalamic region). This distribution is in agreement with previous studies (Buckwalter et al., 2008; Schmahmann and Pandya, 1990; Yeterian and Pandya, 1985), with small differences noted; for example, in the presence of labelled cells in the LD nucleus.

The ventral nuclei and the mediodorsal nucleus receive input from the cerebellum and the basal ganglia, and send their main output to the frontal cortex (Alexander et al. 1991; Asanuma et al. 1983; Kultas-Ilinsky et al. 2003; McFarland and Haber 2002; Mitchell 2015). Through posterior parts of the VL nucleus (the postrema, VLps, and caudal, VLc, divisions), PGm appears to receive primarily cerebellar influences (Asanuma et al. 1983; Stepniewska et al. 2003) or a balance of cerebellar–pallidal influences, according to other studies (Rouiller et al. 1994). The dorsal–posterior part of VL is the dominant source of input to medial and caudal parietal areas (Schmahmann and Pandya 1990; Gamberini et al. 2016; Impieri et al. 2018); the parietal projection zone is much restricted compared to the wider territory of the lateral thalamic region that sends projections to motor and premotor areas (Matelli and Luppino 1996; Morel et al. 2005; Burman et al. 2014a, b). In addition, the role of VLc/VLps in motor behavior is unclear given that the majority of responses in this region occur after passive somatosensory stimulation (Vitek et al. 1994) and microstimulation of the dorsal VL has little effect in producing movement (Vitek et al. 1996).

The functions of medial, intralaminar and limbic connections of PGm are less clear. Prevalent theories suggest they might be associated with the arousal and visual awareness systems (Purpura and Schiff 1997), with spatial learning and memory (Aggleton and Nelson 2015) and the temporal propagation of cortical activity (Pergola et al. 2018). Several aspects of these behaviors might be mediated by eye movements, as suggested by the presence of neurons in the medial and central thalamus that show oculomotor, fixation, and eye-position activations (Schlag and Schlag-Rey 1984; Schlag-Rey and Schlag 1984; Watanabe and Funahashi 2004; Tanaka 2005).

Conclusions

Several lines of evidence in humans, including results from resting-state functional connectivity and morphological analyses (Cauda et al. 2010; Pereira-Pedro and Bruner 2016; Bruner et al. 2017) as well as comparative imaging studies between humans and macaques (Margulies et al. 2009), suggest that the caudomedial lobe contains several functional modules, although the specifics of the extent and roles for each functional entity remain to be fully characterized (Cauda et al. 2010).

Architectural studies in macaque monkeys (Morecraft et al. 2004; Luppino et al. 2005) have described a series of areas in the caudomedial lobe and their cortico-cortical connections (Cavada and Goldman-Rakic 1989a, b; Parvizi et al. 2006; Gamberini et al. 2016; Passarelli et al. 2018). Our present results and previous findings (Schmahmann and Pandya 1990; Buckwalter et al. 2008; Gamberini et al. 2016; Impieri et al. 2018) show that although the caudomedial lobe is a major site of converging subcortical projections from the posterior thalamus, there is specificity in the projections from the various subdivisions of the pulvinar. Thus, dorsorostral parts of medial parietal cortex (areas 31 and PEci) are targeted by the oral pulvinar; the caudal medial lobe, including the core of the precuneus (PGm), V6A, and PEc, much like the caudal inferior parietal cortex and the posterior cingulate cortex, receives substantial projections from the medial pulvinar, in particular from its dorsal part. The origins of projections are different for each region: those directed to parietal cortex stem from lateral and central locations; projections to cingulate cortex also arise from medial locations. The ventral and caudal part of the medial lobe, corresponding to the parieto-occipital area V6, receives its major input from "visual' parts of the pulvinar, i.e., the inferior and lateral subdivisions. In a broad sense, these data conform to a general role for the dorsal caudomedial lobe in the guidance of sensory-spatial behavior, whereas the ventral caudalmost region forms part of the visual networks of the brain. Future studies designed to map the sensory properties of pulvinar populations are necessary to understand in more detail the role of these specific pulvinar-cortical networks in shaping primate and human motor functions and cognition.

Acknowledgements We thank K. E. Richardson, M. Verdosci, and F. Campisi for expert technical assistance and C. Cranfield for proofreading the manuscript.

Funding Australian Research Council (CE140100007, DE120102883, DP140101968), National Health and Medical Research Council (1020839, 1082144), European Union Grant FP7-ICT 217077-EYESHOTS, FP7-PEOPLE-2011-IOF 300452 (S.B.), H2020-MSCA-734227-PLATYPUS and Ministero dell'Università e della Ricerca (2015AWSW2Y_001, 2017KZNZLN), and Fondazione del Monte di Bologna e Ravenna, Italy.

Compliance with ethical standards

Conflict of interest The authors declare that they have no conflict of interest.

References

Acuña C, Cudeiro J, Gonzalez F (1986) Lateral-posterior (LP) and pulvinar unit activity related to intentional upper limb movements directed to spatially separated targets, in behaving *Macaca nemestrina* monkeys. Rev Neurol (Paris) 142:354–361

Acuña C, Cudeiro J, Gonzalez F et al (1990) Lateral-posterior and pulvinar reaching cells—comparison with parietal area 5a: a study in behaving *Macaca nemestrina* monkeys. Exp Brain Res 82:158–166. https://doi.org/10.1007/BF00230847

Aggleton JP, Nelson AJD (2015) Why do lesions in the rodent anterior thalamic nuclei cause such severe spatial deficits? Neurosci Biobehav Rev 54:131–144

Alexander GE, Crutcher MD, DeLong MR (1991) Basal ganglia-thalamocortical circuits: parallel substrates for motor, oculomotor, "prefrontal" and "limbic" functions, Chapter 6. In: Uylings HBM, Eden CG, Bruin JPC, et al. (eds) The prefrontal its structure, function and cortex pathology. Elsevier, Amsterdam, pp 119–146

Andersen RA, Andersen KN, Hwang EJ, Hauschild M (2014) Optic ataxia: from Balint's syndrome to the parietal reach region. Neuron 81:967–983. https://doi.org/10.1016/j.neuron.2014.02.025

Asanuma C, Thach WT, Jones EG (1983) Distribution of cerebellar terminations and their relation to other afferent terminations in the ventral lateral thalamic region of the monkey. Brain Res Rev 5:237–265. https://doi.org/10.1016/0165-0173(83)90015-2

Baleydier C, Morel A (1992) Segregated thalamocortical pathways to inferior parietal and inferotemporal cortex in macaque monkey. Vis Neurosci 8:391–405. https://doi.org/10.1017/S0952523800004922

Battaglia-Mayer A, Ferraina S, Genovesio A et al (2001) Eye-hand coordination during reaching. II. An analysis of the relationships between visuomanual signals in parietal cortex and parieto-frontal association projections. Cereb Cortex 11:528–544. https://doi.org/10.1093/cercor/11.6.528

Battaglini PP, Muzur A, Galletti C et al (2002) Effects of lesions to area V6A in monkeys. Exp brain Res 144:419–422. https://doi.org/10.1007/s00221-002-1099-4

Baumann O, Chan E, Mattingley JB (2012) Distinct neural networks underlie encoding of categorical versus coordinate spatial relations during active navigation. Neuroimage 60:1630–1637. https://doi.org/10.1016/j.neuroimage.2012.01.089

Boussaoud D, Desimone R, Ungerleider LG (1992) Subcortical connections of visual areas MST and FST in macaques. Vis Neurosci 9:291–302. https://doi.org/10.1017/S0952523800010701

Bruner E, Pereira-Pedro AS, Chen X, Rilling JK (2017) Precuneus proportions and cortical folding: a morphometric evaluation on a racially diverse human sample. Ann Anat 211:120–128. https://doi.org/10.1016/j.aanat.2017.02.003

Buckner RL, Snyder AZ, Sanders AL et al (2000) Functional brain imaging of young, nondemented, and demented older adults. J Cogn Neurosci 12:24–34. https://doi.org/10.1162/089892900564046

Buckner RL, Snyder AZ, Shannon BJ et al (2005) Molecular, structural, and functional characterization of Alzheimer's disease: evidence for a relationship between default activity, amyloid, and memory. J Neurosci 25:7709–7717

Buckwalter JA, Parvizi J, Morecraft RJ, Van Hoesen GW (2008) Thalamic projections to the posteromedial cortex in the macaque. J Comp Neurol 507:1709–1733. https://doi.org/10.1002/cne.21647

Burman KJ, Bakola S, Richardson KE et al (2014a) Patterns of afferent input to the caudal and rostral areas of the dorsal premotor cortex (6DC and 6DR) in the marmoset monkey. J Comp Neurol 522:3683–3716. https://doi.org/10.1002/cne.23633

Burman KJ, Bakola S, Richardson KE et al (2014b) Patterns of cortical input to the primary motor area in the marmoset monkey. J Comp Neurol 522:811–843. https://doi.org/10.1002/cne.23447

Cappe C, Morel A, Rouiller EM (2007) Thalamocortical and the dual pattern of corticothalamic projections of the posterior parietal cortex in macaque monkeys. Neuroscience 146:1371–1387. https://doi.org/10.1016/j.neuroscience.2007.02.033

Cauda F, Geminiani G, D'Agata F et al (2010) Functional connectivity of the posteromedial cortex. PLoS ONE 5:e13107. https://doi.org/10.1371/journal.pone.0013107

Cavada C, Goldman-Rakic PS (1989a) Posterior parietal cortex in rhesus monkey: II. Evidence for segregated corticocortical networks linking sensory and limbic areas with the frontal lobe. J Comp Neurol 287:422–445

Cavada C, Goldman-Rakic PS (1989b) Posterior parietal cortex in rhesus monkey: I. Parcellation of areas based on distinctive limbic and sensory corticocortical connections. J Comp Neurol 287:393–421. https://doi.org/10.1002/cne.902870402

Cavanna AE, Trimble MR (2006) The precuneus: a review of its functional anatomy and behavioural correlates. Brain 129:564–583

Cudeiro J, Gonzalez F, Perez R et al (1989) Does the pulvinar-LP complex contribute to motor programming? Brain Res 484:367–370. https://doi.org/10.1016/0006-8993(89)90383-1

Cunningham SI, Tomasi D, Volkow ND (2017) Structural and functional connectivity of the precuneus and thalamus to the default mode network. Hum Brain Mapp 38:938–956. https://doi.org/10.1002/hbm.23429

Fattori P, Breveglieri R, Bosco A et al (2017) Vision for prehension in the medial parietal cortex. Cereb Cortex 27:1149–1163. https://doi.org/10.1093/cercor/bhv302

Fernández-Espejo D, Soddu A, Cruse D et al (2012) A role for the default mode network in the bases of disorders of consciousness. Ann Neurol 72:335–343. https://doi.org/10.1002/ana.23635

Ferraina S, Garasto MR, Battaglia-Mayer A et al (1997) Visual control of hand-reaching movement: activity in parietal area 7m. Eur J Neurosci 9:1090–1095. https://doi.org/10.1111/j.1460-9568.1997.tb01460.x

Galletti C, Fattori P (2018) The dorsal visual stream revisited: stable circuits or dynamic pathways? Cortex 98:203–217. https://doi.org/10.1016/j.cortex.2017.01.009

Gallyas F (1979) Silver staining of myelin by means of physical development. Neurol Res 1:203–209

Gamberini M, Passarelli L, Fattori P et al (2009) Cortical connections of the visuomotor parietooccipital area V6Ad of the macaque monkey. J Comp Neurol 513:622–642. https://doi.org/10.1002/cne.21980

Gamberini M, Bakola S, Passarelli L et al (2016) Thalamic projections to visual and visuomotor areas (V6 and V6A) in the rostral bank of the parieto-occipital sulcus of the macaque. Brain Struct Funct 221:1573–1589. https://doi.org/10.1007/s00429-015-0990-2

Gamberini M, Dal Bò G, Breveglieri R et al (2018) Sensory properties of the caudal aspect of the macaque superior parietal lobule. Brain Struct Funct 223:1863–1879. https://doi.org/10.1007/s00429-017-1593-x

García-Cabezas MÁ, Rico B, Sánchez-González MÁ, Cavada C (2007) Distribution of the dopamine innervation in the macaque and human thalamus. Neuroimage 34:965–984. https://doi.org/10.1016/j.neuroimage.2006.07.032

Gattass R, Galkin TW, Desimone R, Ungerleider LG (2014) Subcortical connections of area V4 in the macaque. J Comp Neurol 522:1941–1965. https://doi.org/10.1002/cne.23513

Grieve KL, Acuña C, Cudeiro J (2000) The primate pulvinar nuclei: vision and action. Trends Neurosci 23:35–39. https://doi.org/10.1016/S0166-2236(99)01482-4

Hadjidimitrakis K, Dal Bo' G, Breveglieri R et al (2015) Overlapping representations for reach depth and direction in caudal superior parietal lobule of macaques. J Neurophysiol 114:2340–2352. https://doi.org/10.1152/jn.00486.2015

Hadjidimitrakis K, Bakola S, Wong YT, Hagan MA (2019) Mixed spatial and movement representations in the primate posterior parietal cortex. Front Neural Circuits 13:15. https://doi.org/10.3389/fncir.2019.00015

Hardy SGP, Lynch JC (1992) The spatial distribution of pulvinar neurons that project to two subregions of the inferior parietal lobule in the macaque. Cereb Cortex 2:217–230. https://doi.org/10.1093/cercor/2.3.217

Homman-Ludiye J, Bourne JA (2019) The medial pulvinar: function, origin and association with neurodevelopmental disorders. J Anat. https://doi.org/10.1111/joa.12932

Impieri D, Gamberini M, Passarelli L et al (2018) Thalamo-cortical projections to the macaque superior parietal lobule areas PEc and PE. J Comp Neurol 526:1041–1056. https://doi.org/10.1002/cne.24389

Jones EG (2001) The thalamic matrix and thalamocortical synchrony. Trends Neurosci 24:595–601. https://doi.org/10.1016/S0166-2236(00)01922-6

Kaas JH, Lyon DC (2007) Pulvinar contributions to the dorsal and ventral streams of visual processing in primates. Brain Res Rev 55:285–296. https://doi.org/10.1016/j.brainresrev.2007.02.008

Kamishina H, Yurcisin GH, Corwin JV, Reep RL (2008) Striatal projections from the rat lateral posterior thalamic nucleus. Brain Res 1204:24–39. https://doi.org/10.1016/j.brainres.2008.01.094

Kamishina H, Conte WL, Patel SS et al (2009) Cortical connections of the rat lateral posterior thalamic nucleus. Brain Res 1264:39–56. https://doi.org/10.1016/j.brainres.2009.01.024

Kravitz DJ, Saleem KS, Baker CI, Mishkin M (2011) A new neural framework for visuospatial processing. Nat Rev Neurosci 12:217–230. https://doi.org/10.1038/nrn3008

Kultas-Ilinsky K, Sivan-Loukianova E, Ilinsky IA (2003) Reevaluation of the primary motor cortex connections with the thalamus in primates. J Comp Neurol 457:133–158. https://doi.org/10.1002/cne.10539

Leichnetz GR (2001) Connections of the medial posterior parietal cortex (area 7m) in the monkey. Anat Rec 263:215–236

Luppino G, Ben Hamed S, Gamberini M et al (2005) Occipital (V6) and parietal (V6A) areas in the anterior wall of the parieto-occipital sulcus of the macaque: a cytoarchitectonic study. Eur J Neurosci 21:3056–3076. https://doi.org/10.1111/j.1460-9568.2005.04149.x

Lustig C, Snyder AZ, Bhakta M et al (2003) Functional deactivations: change with age and dementia of the Alzheimer type. Proc Natl Acad Sci 100:14504–14509

Mai JK, Forutan F (2012) Thalamus, Chapter 19. In: Mai JK, Paxinos GBT (eds) The human. Academic Press, San Diego, pp 618–677

Margulies DS, Vincent JL, Kelly C et al (2009) Precuneus shares intrinsic functional architecture in humans and monkeys. Proc Natl Acad Sci 106:20069–20074. https://doi.org/10.1073/pnas.0905314106

Matelli M, Luppino G (1996) Thalamic input to mesial and superior area 6 in the macaque monkey. J Comp Neurol 372:59–87. https://doi.org/10.1002/(SICI)1096-9861(19960812)372:1%3c59:AID-CNE6%3e3.0.CO;2-L

Matsuda H (2001) Cerebral blood flow and metabolic abnormalities in Alzheimer's disease. Ann Nucl Med 15:85. https://doi.org/10.1007/BF02988596

McFarland NR, Haber SN (2002) Thalamic relay nuclei of the basal ganglia form both reciprocal and nonreciprocal cortical connections, linking multiple frontal cortical areas. J Neurosci 22:8117–8132. https://doi.org/10.1523/JNEUROSCI.22-18-08117.2002

Mitchell AS (2015) The mediodorsal thalamus as a higher order thalamic relay nucleus important for learning and decision-making. Neurosci Biobehav Rev 54:76–88. https://doi.org/10.1016/j.neubiorev.2015.03.001

Morecraft RJ, Cipolloni PB, Stilwell-Morecraft KS et al (2004) Cytoarchitecture and cortical connections of the posterior cingulate and adjacent somatosensory fields in the rhesus monkey. J Comp Neurol 469:37–69. https://doi.org/10.1002/cne.10980

Morel A, Liu J, Wannier T et al (2005) Divergence and convergence of thalamocortical projections to premotor and supplementary motor cortex: a multiple tracing study in the macaque monkey. Eur J Neurosci 21:1007–1029. https://doi.org/10.1111/j.1460-9568.2005.03921.x

Olson CR, Musil SY, Goldberg ME (1996) Single neurons in posterior cingulate cortex of behaving macaque: eye movement signals. J Neurophysiol 76:3285–3300. https://doi.org/10.1152/jn.1996.76.5.3285

Olszewski J (1952) The thalamus of the Macaca mulatta. In: Karger S (ed) An atlas for use with the stereotaxic instrument. Karger Publishers, Basel, Switzerland, New York

Padberg J, Cerkevich C, Engle J et al (2009) Thalamocortical connections of parietal somatosensory cortical fields in macaque monkeys are highly divergent and convergent. Cereb Cortex 19:2038–2064. https://doi.org/10.1093/cercor/bhn229

Pandya DN, Seltzer B (1982) Intrinsic connections and architectonics of posterior parietal cortex in the rhesus monkey. J Comp Neurol 204:196–210. https://doi.org/10.1002/cne.902040208

Parvizi J, Van Hoesen GW, Buckwalter J, Damasio A (2006) Neural connections of the posteromedial cortex in the macaque. Proc Natl Acad Sci 103:1563–1568

Passarelli L, Rosa MGP, Bakola S et al (2018) Uniformity and diversity of cortical projections to precuneate areas in the macaque monkey: what defines area PGm? Cereb Cortex 28:1700–1717. https://doi.org/10.1093/cercor/bhx067

Pereira-Pedro AS, Bruner E (2016) Sulcal pattern, extension, and morphology of the precuneus in adult humans. Ann Anat 208:85–93. https://doi.org/10.1016/j.aanat.2016.05.001

Pergola G, Danet L, Pitel A-L et al (2018) The regulatory role of the human mediodorsal thalamus. Trends Cogn Sci 22:1011–1025. https://doi.org/10.1016/j.tics.2018.08.006

Petersen SE, Robinson DL, Keys W (1985) Pulvinar nuclei of the behaving rhesus monkey: visual responses and their modulation. J Neurophysiol 54:867–886

Purpura KP, Schiff ND (1997) The thalamic intralaminar nuclei: a role in visual awareness. Neurosci 3:8–15. https://doi.org/10.1177/107385849700300110

Romanski LM, Giguere M, Bates JF, Goldman-Rakic PS (1997) Topographic organization of medial pulvinar connections with the prefrontal cortex in the rhesus monkey. J Comp Neurol 379:313–332. https://doi.org/10.1002/(SICI)1096-9861(19970317)379:3%3c313:AID-CNE1%3e3.0.CO;2-6

Rosa MGP, Palmer SM, Gamberini M et al (2005) Resolving the organization of the New World monkey third visual complex: the dorsal extrastriate cortex of the marmoset (*Callithrix jacchus*). J Comp Neurol 483:164–191

Rouiller EM, Liang F, Babalian A et al (1994) Cerebellothalamocortical and pallidothalamocortical projections to the primary and supplementary motor cortical areas: a multiple tracing study in macaque monkeys. J Comp Neurol 345:185–213

Saalmann YB, Pinsk MA, Wang L et al (2012) The pulvinar regulates information transmission between cortical areas based on attention demands. Science 337:753–756. https://doi.org/10.1126/science.1223082

Sato N, Sakata H, Tanaka YL, Taira M (2006) Navigation-associated medial parietal neurons in monkeys. Proc Natl Acad Sci USA 103:17001–17006. https://doi.org/10.1073/pnas.0604277103

Sato N, Sakata H, Tanaka YL, Taira M (2010) Context-dependent place-selective responses of the neurons in the medial parietal

region of macaque monkeys. Cereb Cortex 20:846–858. https://doi.org/10.1093/cercor/bhp147
Schlag J, Schlag-Rey M (1984) Visuomotor functions of central thalamus in monkey. II. Unit activity related to visual events, targeting, and fixation. J Neurophysiol 51:1175–1195. https://doi.org/10.1152/jn.1984.51.6.1175
Schlag-Rey M, Schlag J (1984) Visuomotor functions of central thalamus in monkey. I. Unit activity related to spontaneous eye movements. J Neurophysiol 51:1149–1174. https://doi.org/10.1152/jn.1984.51.6.1149
Schmahmann JD, Pandya DN (1990) Anatomical investigation of projections from thalamus to posterior parietal cortex in the rhesus monkey: a WGA-HRP and fluorescent tracer study. J Comp Neurol 295:299–326. https://doi.org/10.1002/cne.902950212
Shipp S (2003) The functional logic of cortico–pulvinar connections. Philos Trans R Soc London Ser B Biol Sci 358:1605–1624
Soddu A, Vanhaudenhuyse A, Schnakers C et al (2010) Default network connectivity reflects the level of consciousness in non-communicative brain-damaged patients. Brain 133:161–171. https://doi.org/10.1093/brain/awp313
Stepniewska I, Sakai ST, Qi H, Kaas JH (2003) Somatosensory input to the ventrolateral thalamic region in the macaque monkey: a potential substrate for parkinsonian tremor. J Comp Neurol 455:378–395
Tanaka M (2005) Involvement of the central thalamus in the control of smooth pursuit eye movements. J Neurosci 25:5866–5876. https://doi.org/10.1523/JNEUROSCI.0676-05.2005
Thier P, Andersen RA (1998) Electrical microstimulation distinguishes distinct saccade-related areas in the posterior parietal cortex. J Neurophysiol 80:1713–1735. https://doi.org/10.1152/jn.1998.80.4.1713
Tomasi D, Volkow ND (2011) Association between functional connectivity hubs and brain networks. Cereb Cortex 21:2003–2013
Ungerleider LG, Galkin TW, Desimone R, Gattass R (2014) Subcortical projections of area V2 in the macaque. J Cogn Neurosci 26:1220–1233. https://doi.org/10.1162/jocn_a_00571
Van Essen DC, Lewis JW, Drury HA et al (2001) Mapping visual cortex in monkeys and humans using surface-based atlases. Vision Res 41:1359–1378. https://doi.org/10.1016/s0042-6989(01)00045-1
Vitek JL, Ashe J, DeLong MR, Alexander GE (1994) Physiologic properties and somatotopic organization of the primate motor thalamus. J Neurophysiol 71:1498–1513. https://doi.org/10.1152/jn.1994.71.4.1498
Vitek JL, Ashe J, DeLong MR, Kaneoke Y (1996) Microstimulation of primate motor thalamus: somatotopic organization and differential distribution of evoked motor responses among subnuclei. J Neurophysiol 75:2486–2495
Vogt BA, Laureys S (2005) Posterior cingulate, precuneal and retrosplenial cortices: cytology and components of the neural network correlates of consciousness. Prog Brain Res 150:205–217
Vogt BA, Vogt L, Farber NB, Bush G (2005) Architecture and neurocytology of monkey cingulate gyrus. J Comp Neurol 485:218–239
Watanabe Y, Funahashi S (2004) Neuronal activity throughout the primate mediodorsal nucleus of the thalamus during oculomotor delayed-responses. II. Activity encoding visual versus motor signal. J Neurophysiol 92:1756–1769. https://doi.org/10.1152/jn.00995.2003
Wenderoth N, Debaere F, Sunaert S, Swinnen SP (2005) The role of anterior cingulate cortex and precuneus in the coordination of motor behaviour. Eur J Neurosci 22:235–246. https://doi.org/10.1111/j.1460-9568.2005.04176.x
Wilke M, Kagan I, Andersen RA (2013) Effects of pulvinar inactivation on spatial decision-making between equal and asymmetric reward options. J Cogn Neurosci 25:1270–1283. https://doi.org/10.1162/jocn_a_00399
Wong-Riley M (1979) Changes in the visual system of monocularly sutured or enucleated cats demonstrable with cytochrome oxidase histochemistry. Brain Res 171:11–28. https://doi.org/10.1016/0006-8993(79)90728-5
Yeterian EH, Pandya DN (1985) Corticothalamic connections of the posterior parietal cortex in the rhesus monkey. J Comp Neurol 237:408–426. https://doi.org/10.1002/cne.902370309
Yeterian EH, Pandya DN (1988) Corticothalamic connections of paralimbic regions in the rhesus monkey. J Comp Neurol 269:130–146. https://doi.org/10.1002/cne.902690111
Zhang S, Li CR (2012) Functional connectivity mapping of the human precuneus by resting state fMRI. Neuroimage 59:3548–3562. https://doi.org/10.1016/j.neuroimage.2011.11.023

Publisher's Note Springer Nature remains neutral with regard to jurisdictional claims in published maps and institutional affiliations.